ACS OMEGA

Article

http://pubs.acs.org/journal/acsodf

# Spin-State Patterning in an Iron(II) Tripodal Spin-Crossover Complex

Li Li,[†] Suzanne M. Neville,[‡] Alexander R. Craze,[†] Jack K. Clegg,[§] Natasha F. Sciortino,[‡] Kasun S. Athukorala Arachchige,[§] Outi Mustonen,[∥] Christopher E. Marjo,[∥] Christopher R. McRae,[⊥] Cameron J. Kepert,[‡] Leonard F. Lindoy,[‡] Janice R. Aldrich-Wright,[†] and Feng Li*[,†]

[†]School of Science and Health, Western Sydney University, Locked Bag 1797, Penrith, Sydney, NSW 2751, Australia

[‡]School of Chemistry, University of Sydney, Sydney, NSW 2006, Australia

[§]School of Chemistry and Molecular Biosciences, The University of Queensland, St Lucia, Brisbane, QLD 4072, Australia

[∥]Mark Wainwright Analytical Centre, University of New South Wales, Sydney, NSW 2052, Australia

[⊥]Department of Chemistry and Biomolecular Sciences, Macquarie University, Sydney, NSW 2109, Australia

Supporting Information

**ABSTRACT:** A mononuclear iron(II) complex that displays a gradual two-step spin-crossover (SCO) transition is reported. The intermediate plateau (IP) occurs between $HS^{0.40}LS^{0.60}$ and $HS^{0.30}LS^{0.70}$ (HS = high spin; LS = low spin) ratios over the region of ca. 190−170 K. A phase change occurs at the IP, breaking the symmetry, resulting in six independent SCO sites compared to one at the 100% HS and LS plateau regions, respectively. Variable-temperature X-ray photoelectron spectroscopy shows that the SCO behavior is completely reversible among the HS, IP, and LS regions. The results both confirm and extend the related results for the above system described by Halcrow et al. (Kulmaczewski, R.; Cespedes, O.; Halcrow, M. A. Gradual Thermal Spin-Crossover Mediated By a Reentrant $Z' = 1 \rightarrow Z' = 6 \rightarrow Z' = 1$ Phase Transition, *Inorg. Chem.* **2017**, *56*, 3144−3148) in a recent report.

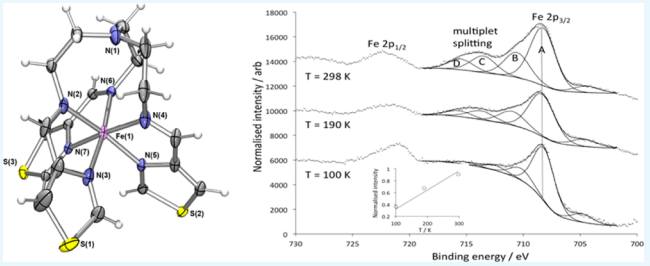


## INTRODUCTION

Spin-crossover (SCO) materials show significant promise for application in several emerging technologies, including molecular switches, sensors, displays, molecular electronics, and spintronics.[1−4] Although a large number of such materials have been developed, leading to a good understanding of the intramolecular properties (choice of metal ion, donor atom, sterics, etc.)[1,2,5−11] that affect spin transitions in discrete complexes, the results of cooperative intramolecular effects (leading to hysteresis, sharp transitions, etc.)[1,2,5,12] are still not readily predictable. This is particularly the case for supramolecular effects involving weak noncovalent interactions and/or crystal packing.[13−18] Extremely recently, Halcrow et al.[19] have reported the crystal structure and SCO properties of $[Fe\mathbf{L}]\cdot(BF_4)_2$ (**L** = tris(2-(((*E*)-thiazol-4-ylmethylene)amino)-ethyl)amine), which features a two-step spin transition together with a symmetry-breaking phase change. Illustrating the immense interest in the field, we had been simultaneously and independently investigating the same material. Our results are largely consistent with those of Halcrow et al.[19] Here, we present complementary results, including the high-resolution crystal structure of the intermediate phase (190 K), that clarify the symmetry-breaking nature of the phase transition: variable-temperature magnetic susceptibility measurements with slow scan rates, and variable-temperature X-ray photoelectron spectroscopy (VT-XPS).

## RESULTS AND DISCUSSION

The $[Fe\mathbf{L}]\cdot(BF_4)_2$ (Figure 1) complex was prepared in a similar manner to that reported by Halcrow et al.,[19] and we prepared single crystals by the slow diffusion of diethyl ether into an acetonitrile solution. The composition and purity of $[Fe\mathbf{L}]\cdot(BF_4)_2$ was established by elemental analysis, high-resolution electrospray ionization mass spectrometry, solid-state UV−vis spectroscopy, IR spectroscopy, and powder X-ray diffraction (see Supporting Information).

Variable-temperature magnetic susceptibility measurements for $[Fe\mathbf{L}]\cdot(BF_4)_2$ revealed the presence of a complete nonhysteretic SCO transition with a two-step character (Figure 2). These results are consistent with those of Halcrow et al.[19] The two-step character arises from a change in slope over the region of ca. 190−170 K, representative of an intermediate plateau (IP) (however with declining rather than stable $\chi_M T$ values). At 190 K, the $\chi_M T$ value of ca. 1.25 $cm^3\ mol^{-1}\ K$ corresponds to a high spin (HS)/low spin (LS) ratio of ca. 40:60 of Fe(II) sites, which drops to an HS/LS ratio of ca. 30:70 by 170 K.

VT-XPS (Figure 3 and see Supporting Information) showed the expected changes arising from the spin state on the Fe $2p_{3/2}$

**Received:** May 18, 2017
**Accepted:** June 23, 2017
**Published:** July 10, 2017

  

DOI: 10.1021/acsomega.7b00630
*ACS Omega* 2017, 2, 3349−3353

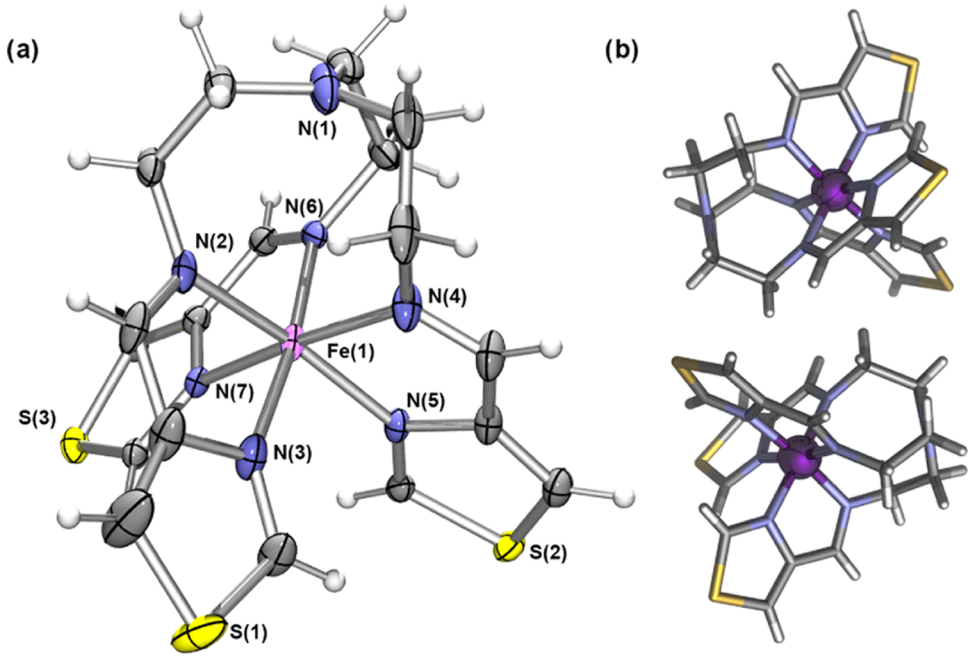


**Figure 1.** (a) Oak Ridge thermal ellipsoid plot (50% probability ellipsoids) of $[FeL]\cdot(BF_4)_2$ at 100 K (anions omitted for clarity). (b) Structural representation of the pairs of $[FeL]^{2+}$ cations (Fe−Fe separation, 7.38 Å). Regions of disorder have been omitted for clarity.

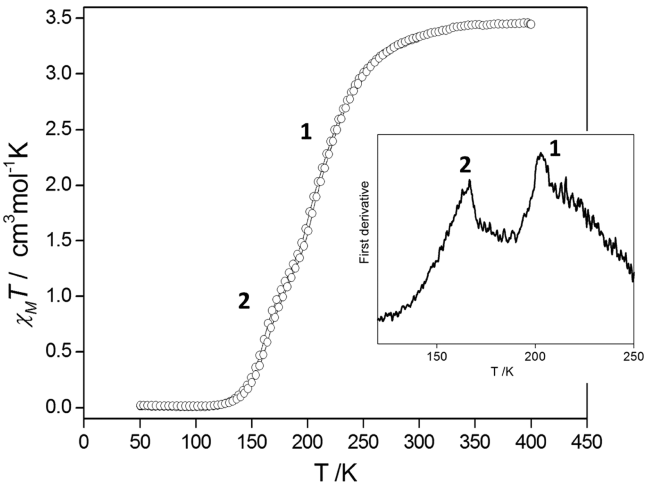


**Figure 2.** Variable-temperature magnetic susceptibility ($\chi_M T$ vs $T$) for $[FeL]\cdot(BF_4)_2$ over the range 400−50−400 K at a scan rate of 2 K min$^{-1}$. Inset: first derivative of the SCO transition highlighting the two-step character (**1** and **2**).

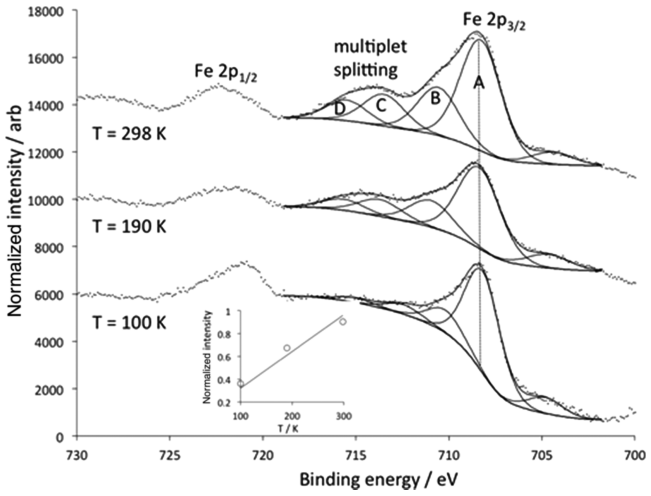


**Figure 3.** VT-XPS of the Fe 2p region.

peak.[20,21] On X-ray ionization, compounds of the 3d transition metals undergo a coupling between the ionized 2p shell and the 3d shell to form multiplets, with an intensity dependent on the number of unpaired electrons in the 3d shell.[22] Hence, the Fe $2p_{3/2}$ peak of the HS complex at 298 K splits into relatively intense multiplets (peaks B−D). On cooling to 190 K, the combined normalized intensity of multiplets B−D decreases (inset in Figure 4), until a typical LS Fe(II) spectrum is observed at 100 K. The spin behavior is completely reversible, with the HS spectrum observed on warming to 298 K.

We also determined single-crystal X-ray structures of the HS state (298 K), the intermediate phase (190 K), and the LS state (100 K) (Table S1). Whereas the HS and LS structures are consistent with Halcrow's results, the previous report on the structure of the symmetry-broken intermediate phase ($Z'$ = 6, compared to $Z'$ = 1 at room and low temperature) determined at 175 K "has relatively low precision, reflecting the size of the model and significant cation and anion disorder, which was only partly resolvable".[19] With careful attention to obtaining a suitable crystal, we were able to obtain data of high quality and without substantial disorder.

Detailed analysis (average Fe−N bond lengths and relative Fe(II) octahedral distortion) reveals two HS (Fe(2) and Fe(3)), two LS (Fe(4) and Fe(6)), and two mixed HS−LS Fe(II) sites (Fe(1) and Fe(5)) at 190 K (Figure 4). The spin-state assignment for the complete HS and LS sites was clear on the basis of the average Fe−N bond lengths and relative octahedral distortion at these sites (Table S1). On the basis of the complete HS and LS values above, respectively, the mixed HS−LS Fe(II) sites (i.e., of short-range crystallographic order) are of more LS character than HS. This assignment of short- and long-range ordered HS and LS states over the six distinct Fe(II) sites correlates well with the 40:60 HS/LS ratio observed



DOI: 10.1021/acsomega.7b00630
ACS Omega 2017, 2, 3349−3353

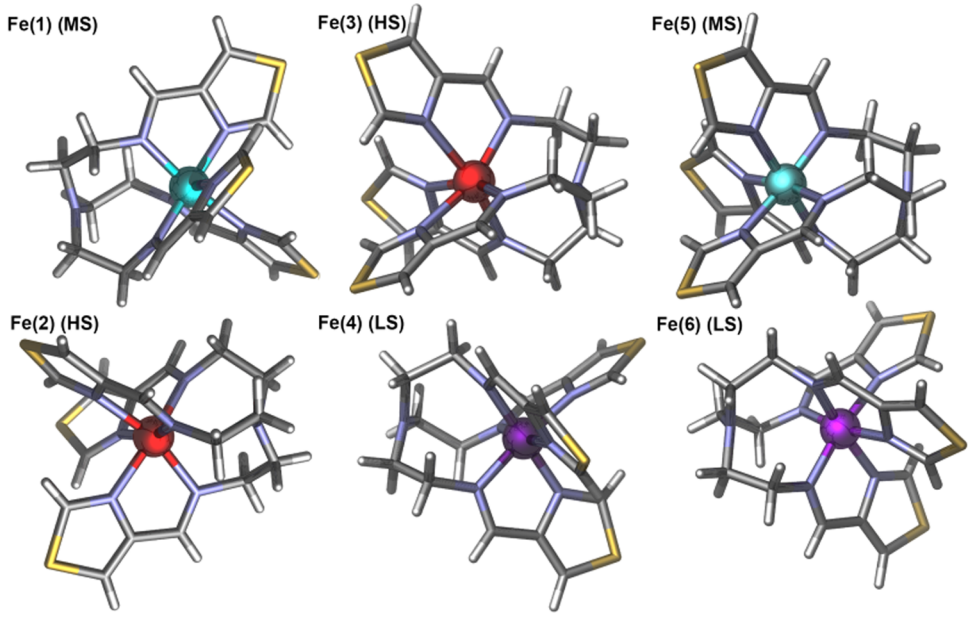


**Figure 4.** Structural representation of the six crystallographically distinct $[FeL]^{2+}$ moieties, which associate into three interacting pairs. Relative spin states of the Fe(II) sites indicated (HS: red, LS: purple, and mixed HS−LS: cyan. Anions and regions of disorder have been omitted for clarity).

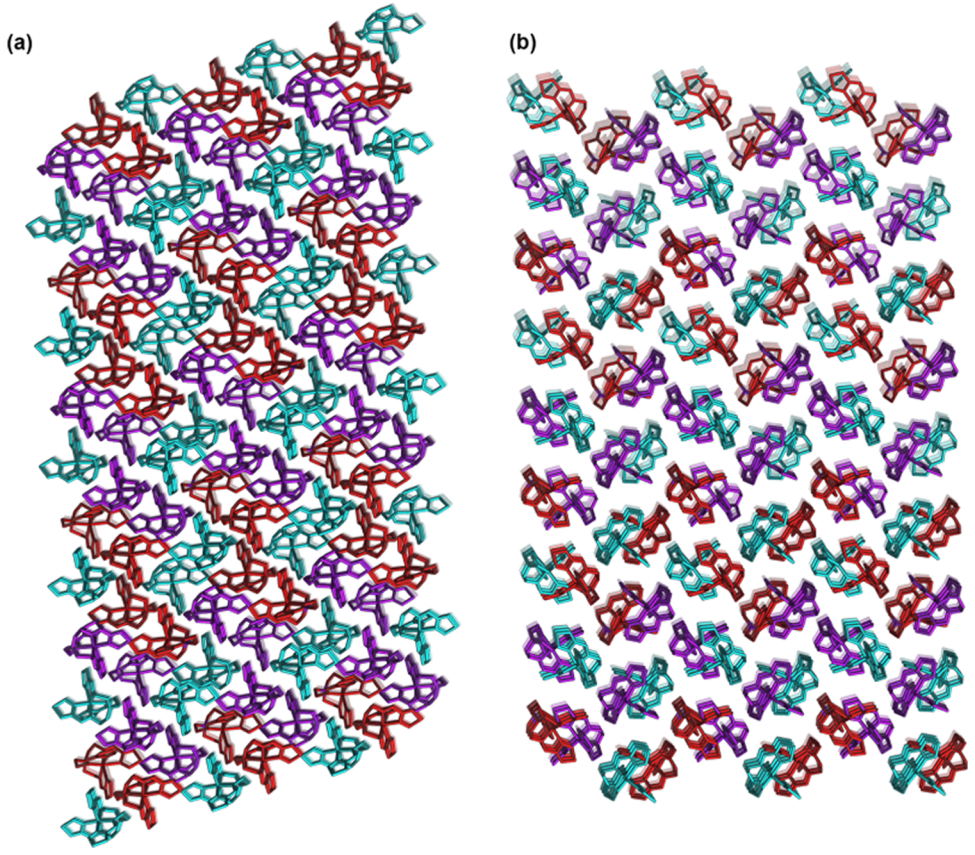


**Figure 5.** Packing diagram illustrating the distribution of the three distinct spin states in the lattice (HS: red, LS: purple, and mixed HS−LS: cyan). Anions, hydrogens, and regions of disorder have been omitted for clarity) viewed along the (a) *a*-direction and (b) *c*-direction.

magnetically at this temperature (Figure 2). We note that the detailed structural analysis reported on this phase by Halcrow et al. was conducted at 175 K, revealing three LS, one HS, and two mixed HS−LS Fe(II) sites, representative of a 30:70 HS/LS ratio as per magnetic measurements. From this, it is interesting then to observe that one of the mixed HS + LS sites attains a complete LS character over the duration of the "sloped" IP temperature range (i.e., 190−170 K).

The $[FeL]^{2+}$ cations at 190 K are arranged in three distinct dimers comprising two mixed spin-state pairs (HS−LS) and one LS state pair (LS−LS) (Figure 4). These three unique pairs are distributed in distinct one-dimensional (1D) chains along



DOI: 10.1021/acsomega.7b00630
*ACS Omega* 2017, 2, 3349−3353

the *a*-direction, as illustrated in Figure 5. Spin-state/dimer confinement is also evident when viewed along the *b*-direction (Figure 5b). The origin for the molecular arrangement of Fe(II) spin states along the 1D chains is likely driven by lattice cooperativity, which arises from packing and short spin-center separations. This produces molecular-level spin-state domain formation within the 1D chains, which is conferred to a 3D spin-state patterning.

## CONCLUSIONS

We have verified the findings of Halcrow et al.,[19] which describe a new discrete mononuclear Fe(II) tripodal complex that displays a two-step SCO behavior. At the intermediate phase, six independent spin sites are present, resulting in 3D spin-state patterning. Although there are no particular structural features and/or interactions that obviously contribute to this distinctive phase transition and rare spin-state patterning, we note that the overall strain involved in the hexadentate ligand type to accommodate the HS to LS transition may be a contributing factor.

## METHODS

**Materials.** All chemicals and solvents used were of commercial grade and used without further purification.

**Experimental Section.** **L** Tris(2-aminoethyl)-amine (104 mg, 0.71 mmol) in 10 mL of ethanol was added to a solution of thiazole-4-carboxaldehyde (250 mg, 2.21 mmol) in 10 mL of ethanol, leading to the formation of a clear yellow solution. The mixture was heated at reflux for 3 h, and then the resulting yellow solution was left at 70 °C with overnight stirring. The residue obtained after the removal of the solvent was dissolved in acetonitrile for recrystallization. The crystallized product was washed with cold acetonitrile (3 × 5 mL) to give a light yellow solid in 67% yield. $^{1}$H NMR ($CDCl_3$, 300 MHz) $\delta$ (ppm): 8.79 (d, 3H), 8.39 (s, 3H), 7.72 (d, 3H), 3.73 (t, 6H, $-CH_2-$), 2.96 (t, 6H, $-CH_2-$); $^{13}$C NMR (dimethyl sulfoxide (DMSO), 75.5 MHz) $\delta$ (ppm): 155.63, 154.63, 153.15, 119.73, 60.08 ($-CH_2-$), 55.43 ($-CH_2-$); UV−vis (solid state in nujol): $\lambda_{max}$ 256 nm; FT-IR (ATR $\nu_{max}$, $cm^{-1}$): 3024, 2926, 2844, 2809, 1650, 1460, 1427, 1408, 1342, 1294, 1240, 1149, 1071, 1021, 938, 883, 858, 822, 755, 557, 491, 458, 413; ESI-HRMS (positive-ion detection, EtOH): $m/z$ = 454.0942 $[Na + L]^+$.

$[FeL](BF4)_2$ (**1**) Iron(II) tetrafluoroborate hexahydrate (41 mg, 0.12 mmol) in 10 mL of acetonitrile was slowly added to a suspension of **L** (50 mg, 0.12 mmol) in 10 mL of acetonitrile; there was an immediate color change from yellow to red. The reaction mixture was heated at 50 °C with stirring for 4 h and then cooled to room temperature and filtered. Slow diffusion of diethyl ether into the filtrate of the product resulted in the formation of dark orange crystals in 83% yield, which were air dried. UV−vis (solid state in nujol): $\lambda_{max}$ 256, 368, 476 nm; FT-IR (ATR $\nu_{max}$, $cm^{-1}$): 3104, 2860, 1633, 1438, 1329, 1285, 1243, 1030, 965, 903, 877, 844, 772, 571, 521, 488; ESI-HRMS (positive-ion detection, $CH_3CN$): $m/z$ = 543.5168 $[Fe + L]^{2+}$ and 574.0453 $[Fe + L + BF_4^-]^+$. Single crystals were taken from the same sample and used directly for the X-ray study.

## ASSOCIATED CONTENT

### Supporting Information

The Supporting Information is available free of charge on the ACS Publications website at DOI: 10.1021/acsomega.7b00630.

Crystallographic data (CIF) (CIF) (CIF)

Additional experimental details on the characterization and physical property measurements of ligand **L** and $[FeL]\cdot(BF_4)_2$ (PDF)

## AUTHOR INFORMATION


### Corresponding Author

*E-mail: feng.li@westernsydney.edu.au.

### ORCID

Suzanne M. Neville: 0000-0003-4237-4046

Jack K. Clegg: 0000-0002-7140-5596

Feng Li: 0000-0001-8465-9678


### Notes

The authors declare no competing financial interest.

## ACKNOWLEDGMENTS

The research described herein was supported by the University of Western Sydney (UWS). The authors acknowledge AMCF and Mass Spectrometry facilities at WSU and MX1 beamline at the Australian Synchrotron. L.L. also acknowledges receipt of an Australian Post-graduate Award and a UWS Top-up Award. A.R.C. acknowledges the award of an AINSE Honours scholarship.

## REFERENCES


(1) *Spin-Crossover Materials: Properties and Applications*; Halcrow, M. A., Ed.; Wiley, 2013.

(2) *Spin Crossover in Transition Metal Compounds I, II and III*; Gütlich, P., Goodwin, H. A., Eds.; Springer, 2004.

(3) Bousseksou, A.; Molnár, G.; Salmon, L.; Nicolazzi, W. Molecular spin crossover phenomenon: recent achievements and prospects. *Chem. Soc. Rev.* **2011**, *40*, 3313−3335.

(4) Kahn, O.; Martinez, C. J. Spin-Transition polymers: from molecular materials toward memory devices. *Science* **1998**, *279*, 44−48.

(5) Ortega-Villar, N.; Muñoz, M. C.; Real, J. A. Symmetry breaking in Iron(II) spin-crossover molecular crystals. *Magnetochemistry* **2016**, *2*, 16.

(6) Li, L.; Saigo, N.; Zhang, Y.; Fanna, D. J.; Shepherd, N. D.; Clegg, J. K.; Zheng, R.; Hayami, S.; Lindoy, L. F.; Aldrich-Wright, J. R.; Li, C.-G.; Reynolds, J. K.; Harman, D. G.; Li, F. A large spin-crossover $[Fe_4L_4]^{8+}$ tetrahedral cage. *J. Mater. Chem. C* **2015**, *3*, 7878−7882.

(7) Matsumoto, T.; Newton, G. N.; Shiga, T.; Hayami, S.; Matsui, Y.; Okamoto, H.; Kumai, R.; Murakami, Y.; Oshio, H. Programmable spin-state switching in a mixed-valence spin-crossover iron grid. *Nat. Commun.* **2014**, *5*, No. 3865.

(8) Duriska, M. B.; Neville, S. M.; Moubaraki, B.; Cashion, J. D.; Halder, G. J.; Chapman, K. W.; Balde, C.; Létard, J.-F.; Murray, K. S.; Kepert, C. J.; Batten, S. R. A nanoscale molecular switch triggered by thermal, light, and guest perturbation. *Angew. Chem., Int. Ed.* **2009**, *48*, 2549−2552.

(9) Nihei, M.; Shiga, T.; Maeda, Y.; Oshio, H. Spin crossover iron(III) complexes. *Coord. Chem. Rev.* **2007**, *251*, 2606−2621.

(10) Halder, G. J.; Kepert, C. J.; Moubaraki, B.; Murray, K. S.; Cashion, J. D. Guest-dependent spin crossover in a nanoporous molecular framework material. *Science* **2002**, *298*, 1762−1765.

(11) Gütlich, P.; Garcia, Y.; Goodwin, H. A. Spin crossover phenomena in Fe(II) complexes. *Chem. Soc. Rev.* **2000**, *29*, 419−427.

(12) Murphy, M. J.; Zenere, K. A.; Ragon, F.; Southon, P. D.; Kepert, C. J.; Neville, S. M. Guest programmable multistep spin crossover in a porous 2-D Hofmann-type material. *J. Am. Chem. Soc.* **2017**, *139*, 1330−1335.

(13) Phonsri, W.; Davies, C. G.; Jameson, G. N. L.; Moubaraki, B.; Ward, J. S.; Kruger, P. E.; Chastanet, G.; Murray, K. S. Symmetry breaking above room temperature in an Fe(II) spin crossover complex with an $N_4O_2$donor set. *Chem. Commun.* **2017**, *53*, 1374−1377.




DOI: 10.1021/acsomega.7b00630
*ACS Omega* 2017, 2, 3349−3353

(14) Sciortino, N. F.; Zenere, K. A.; Corrigan, M. E.; Halder, G. J.; Chastanet, G.; Létard, J.-F.; Kepert, C. J.; Neville, S. M. Four-step iron(II) spin state cascade driven by antagonistic solid state interactions. *Chem. Sci.* **2017**, *8*, 701−707.
(15) Griffin, M.; Shakespeare, S.; Shepherd, H. J.; Harding, C. J.; Létard, J.-F.; Desplanches, C.; Goeta, A. E.; Howard, J. A. K.; Powell, A. K.; Mereacre, V.; Garcia, Y.; Naik, A. D.; Müller-Bunz, H.; Morgan, G. G. A symmetry-breaking spin-state transition in Iron(III). *Angew. Chem., Int. Ed.* **2011**, *50*, 896−900.
(16) Bréfuel, N.; Collet, E.; Watanabe, H.; Kojima, M.; Matsumoto, N.; Toupet, L.; Tanaka, K.; Tuchagues, J.-P. Nanoscale self-hosting of molecular spin-states in the intermediate phase of a spin-crossover material. *Chem. − Eur. J.* **2010**, *16*, 14060−14068.
(17) Struch, N.; Wagner, N.; Schnakenburg, G.; Weisbarth, R.; Klos, S.; Beck, J.; Lützen, A. Thiazolylimines as novel ligand-systems for spin-crossover centred near room temperature. *Dalton Trans.* **2016**, *45*, 14023−14029.
(18) Abedi, A.; Safari, N.; Amani, V.; Khavasi, H. R. Synthesis, characterization, mechanochromism and photochromism of $[Fe(dm4bt)_3][FeCl_4]_2$ and $[Fe(dm4bt)_3][FeBr_4]_2$, along with the investigation of steric influence on spin state. *Dalton Trans.* **2011**, *40*, 6877−6885.
(19) Kulmaczewski, R.; Cespedes, O.; Halcrow, M. A. Gradual thermal spin-crossover mediated by a reentrant $Z' = 1 \rightarrow Z' = 6 \rightarrow Z' = 1$ phase transition. *Inorg. Chem.* **2017**, *56*, 3144−3148.
(20) Burger, K.; Ebel, H.; Madeja, K. The effect of spin states of iron(II) on the XPS of its mixed complexes. *J. Electron Spectrosc. Relat. Phenom.* **1982**, *28*, 115−121.
(21) Beniwal, S.; Zhang, X.; Mu, S.; Naim, A.; Rosa, P.; Chastanet, G.; Létard, J. F.; Liu, J.; Sterbinsky, G. E.; Arena, D. A.; Dowben, P. A.; Enders, A. Surface-induced spin state locking of the $[Fe(H_2B(pz)_2)_2(bipy)]$ spin crossover complex. *J. Phys.: Condens. Matter* **2016**, *28*, No. 206002.
(22) Pronschinske, A.; Bruce, R. C.; Lewis, G.; Chen, Y.; Calzolari, A.; Buongiorno-Nardelli, M.; Shultz, D. A.; You, W.; Dougherty, D. B. Iron(II) spin crossover films on Au(111): scanning probe microscopy and photoelectron spectroscopy. *Chem. Commun.* **2013**, *49*, 10446−10452.



DOI: 10.1021/acsomega.7b00630
*ACS Omega* 2017, 2, 3349−3353